ISSN 0003-6838, Applied Biochemistry and Microbiology, 2018, Vol. 54, No. 4, pp. 379–386. © Pleiades Publishing, Inc., 2018.
Original Russian Text © A.P. Bonartsev, V.V. Voinova, E.S. Kuznetsova, I.I. Zharkova, T.K. Makhina, V.L. Myshkina, D.V. Chesnokova, K.S. Kudryashova, A.V. Feofanov, K.V. Shaitan, G.A. Bonartseva, 2018, published in Prikladnaya Biokhimiya i Mikrobiologiya, 2018, Vol. 54, No. 4.

BSA Adsorption on Porous Scaffolds Prepared from BioPEGylated Poly(3-Hydroxybutyrate)

A. P. Bonartsev[a, b], V. V. Voinova[a, b, *], E. S. Kuznetsova[b], I. I. Zharkova[b], T. K. Makhina[a], V. L. Myshkina[a], D. V. Chesnokova[b], K. S. Kudryashova[b], A. V. Feofanov[b], K. V. Shaitan[b], and G. A. Bonartseva[a]

[a] *Bach Institute of Biochemistry, Federal Research Centre "Fundamentals of Biotechnology" of the Russian Academy of Sciences, Moscow, 119071 Russia*

[b] *Faculty of Biology, Moscow State University, Moscow, 119234 Russia*

**e-mail: veravoinova@mail.ru*

Received November 20, 2017

Abstract—Porous scaffolds for tissue engineering have been prepared from poly(3-hydroxybutyrate) (PHB) and a copolymer of poly(3-hydroxybutyrate) and polyethylene glycol (PHB-PEG) produced by bioPEGylation. The morphology of the scaffolds and their capacity for adsorption of the model protein bovine serum albumin (BSA) have been studied. Scaffolds produced from bioPEGylated PHB adsorbed more BSA, whereas the share of protein irreversibly adsorbed on these scaffolds was significantly lower (33%) than in the case of PHB homopolymer-based scaffolds (47%). The effect of protein adsorption on scaffold biocompatibility in vitro was tested in an experiment that involved the cultivation of fibroblasts (line COS-1) on the scaffolds. PHB-PEG scaffolds had a higher capacity for supporting cell growth than PHB-based scaffolds. Thus, the bioPEGylated PHB-based polymer scaffolds developed in the present study have considerable potential for use in soft tissue engineering.

Keywords: poly(3-hydroxybutyrate), bovine serum albumin, bioPEGylation, polyethylene glycol, adsorption

DOI: 10.1134/S0003683818040038

INTRODUCTION

Poly(3-hydroxyalkanoates) (PHAs) are biocompatible and biodegradable polymers of bacterial origin. They hold considerable potential for use in tissue engineering and regenerative medicine. The homopolymer poly(3-hydroxybutyrate) (PHB**)** is a precursor of all PHAs and the most thoroughly characterized member of this class of polymers. Tissue engineering and the development of medical products for dentistry, orofacial surgery, orthopedics, cardiovascular surgery, hernioplasty, and plastic surgery are promising areas for PHB use. PHB and copolymers thereof are used in tissue engineering as materials for porous 3D-scaffolds that support volume growth of different types of cells, including mesenchymal stem cells, and thus serve as frameworks for hybrid constructs that act as artificial prototypes of living tissues [1, 2]. However, certain PHB properties, such as rather high hydrophobicity, can severely restrict the use of this biopolymer in certain areas, including the development of medical products for reconstructive surgery of soft tissues and cardiovascular surgery [3, 4]. We previously developed a technology for controlled biosynthesis of PHB and its copolymers by the highly efficient *Azotobacter chroococcum* strain 7B. This technology enabled the production of polymers characterized by a high degree of purity and a controlled monomer composition and molecular weight. The group of developed methods included bioPEGylation, i.e., microbiological synthesis of a PHB copolymer with synthetic polyethylene glycol (PEG) added to the cultivation medium of the PHB-producing strain [5, 6]. PEG is a hydrophilic polymer; bioPEGylation therefore reduces the hydrophobicity of the natural biopolymer, making it possible to expand the area of biosynthetic PHA application. BioPEGylation is an alternative to chemical copolymerization techniques and the production of PHB composites with hydrophilic polymers in order to increase PHA hydrophilicity and thus improve polymer compatibility with certain cells and tissues (soft connective tissues, nerve tissue, and blood) [3, 5, 7–10].

Protein adsorption on the polymer surface is a key parameter that determines polymer biocompatibility (cytotoxicity, cell adhesion and proliferation in vitro, hemocompatibility, and compatibility with living tissues upon in vivo implantation). This parameter is especially important in the case of three-dimensional tissue engineering scaffolds produced from PHB and PHB copolymers, since cell adhesion to the inner surface of biopolymer scaffold pores and the subsequent

cell growth largely depend on the formation of an adsorbed protein layer on the polymer surface. Plasma serum albumin plays a key role in protein adsorption, since this protein is the most abundant in blood plasma and tissue fluid at 40–55 g/L, whereas the total protein content is 60–80 g/L. Serum albumin, usually BSA or human serum albumin (HSA) with properties only slightly different from those of BSA, is widely used for tests of protein adsorption on various polymer biomaterials [11]. Moreover, certain researchers assume that the transport of most endogenous PHBs of low molecular weight in the human blood is mediated by serum albumin that binds the polymer noncovalently [12]. Unfortunately, this issue does not always receive sufficient attention in research on PHB and its copolymers, regardless of the existence of scientific publications dedicated to the study of BSA interactions with PHAs. We demonstrated earlier the possibility of microfiber scaffold production from a composite of BSA and a PHB copolymer with 3-hydroxyvalerate (PHBV) by electroformation and studied the release of protein from this construct [13]. Other researchers produced composite micro- and nanoparticles of PHBV and BSA for prolonged protein release [14–16]. Thus, BSA can interact with PHB and its copolymers, but studies of protein adsorption on porous scaffolds for tissue engineering are extremely rare, and protein adsorption on bioPEGylated PHB has not been investigated at all.

The goal of the present study was to investigate the effect of PHB bioPEGylation on the properties of 3D-scaffolds produced from the modified polymer, especially on BSA adsorption on the scaffolds.

MATERIALS AND METHODS

Reagents. Sodium valerate (SV), polyethylene glycol 300 (PEG 300), sodium acetate (SA), inorganic components of the culture medium ($K_2HPO_4 \cdot 3H_2O$, $MgSO_4 \cdot 7H_2O$, NaCl, $Na_2MoO_4 \cdot 2H_2O$, $CaCO_3$, $FeSO_4 \cdot 7H_2O$, $CaCl_2$, KH_2PO_4), sodium citrate, sucrose, agar, and phosphate-buffered saline (PBS) were from Sigma Aldrich (Germany).

Polymer biosynthesis. The highly efficient PHB-producing strain *Azotobacter chroococcum* 7B was used for polymer biosynthesis. This nonsymbiotic, nitrogen-fixing bacterium is capable of polymer superproduction (up to 80% of dry weight of the cells) [6]. The strain was isolated from wheat rhizosphere (sod-podzol soil) and maintained on Ashby medium of the following composition (g/L): $K_2HPO_4 \cdot 3H_2O$, 0.2; $MgSO_4 \cdot 7H_2O$, 0.2; NaCl, 0.2; $Na_2MoO_4 \cdot 2H_2O$, 0.006; $CaCO_3$, 5.0; sucrose, 20; and agar, 20. High cell productivity was attained by means of *Azotobacter chroococcum* cultivation in flasks on an Innova 43 shaker (New Brunswick Scientific, United States) at 250 rpm and 30°C in Burk's medium with the carbon source added in excess. Medium composition was the following (g/L): $MgSO_4 \cdot 7H_2O$—0.4, $FeSO_4 \cdot 7H_2O$—0.01, $Na_2MoO_4 \cdot 2H_2O$—0.006, sodium citrate–0.5, $CaCl_2$—0.1, $K_2HPO_4 \cdot 3H_2O$—1.05, KH_2PO_4—0.2, and sucrose (the main carbon source)—17 (50 mM). Each flask contained 200 mL of medium. The biotechnological PEGylation procedure used for the synthesis of a PHB-PEG copolymer involved supplementation of the producing-strain cultivation medium by PEG 300, a precursor for copolymer biosynthesis. PEG 300 (final concentration 150 mM) was added to the cultivation medium 12 h after the beginning of producing-strain cultivation. The PEG concentration and the timing of PEG addition were optimized in an earlier study [6]. Sodium acetate was added to the culture medium according to a previously developed procedure for regulation of the PHB molecular weight (MW) [17]. This procedure enabled the reduction of the PHB homopolymer MW and production of PHB and PHB-PEG polymers with comparable MW values. The producing strain was cultivated for 72 h. Nephelometry was used to control the optical density of culture medium. Cell growth and polymer accumulation were also monitored with a Biomed-1 microscope (Biomed, Russia) connected to a digital camera. Copolymer biosynthesis parameters, namely, biomass yield (g/L medium) and total polymer content in the cells (% of dry cell weight) (Table 1) were measured according to the previously developed procedures [6]. Polymer isolation and purification (starting from the producing-strain biomass) included chloroform extraction, filtering, isopropanol precipitation, purification in several dissolution-precipitation cycles, and drying, as described earlier [6].

Analysis of chemical composition of the polymer by nuclear magnetic resonance (NMR) spectroscopy. The ^1H NMR spectra of 1% (wt/vol) solutions of the polymers in deuterated chloroform were registered by a MSL-300 300 MHz spectrometer (Bruker, Germany) at the following settings: a temperature of 313°K, a relaxation delay of 2.5 s, and a spectral window width of 10000 Hz. Chemical shifts (ppm) were calibrated with the signal of residual protons of $CDCl_3$ (7.24 ppm relatively to TMS). The relative content of ethylene glycol (EG) elementary units in the PHB-PEG copolymer was calculated with the ratio of the sum of signal intensity for $-CH_2-$ groups of EG (3.61, 3.70, 3.66, 3.73, and 4.24 ppm) and the methyl group of 3-hydroxybutyrate (1.27 ppm) [6].

Assessment of molecular weight of the polymers. The molecular weights of PHB and PHB-PEG were assessed by capillary viscometry in a VPZh-1 glass capillary viscometer (capillary diameter 0.34 mm, Novolab, Russia). The viscosity was measured at a temperature of 30±0.5°C. The polymer concentration in the studied samples was 100–190 mg polymer per 100 mL chloroform. The specific viscosity was calculated according to the formula:

$$\eta_{sp} = (t - t_0)/t_0,$$

Table 1. Biosynthesis conditions and characteristics of PHB and a PHB-PEG copolymer produced by bioPEGylation

Polymers	Cultivation conditions and parameters of producing strain growth			Physicochemical properties of the polymers			
	substrate, (concentration/time of addition)	biomass yield, g/L ± SD	total polymer content, % ± SD	MW, $\times 10^5$ Da	EG content, mol %	contact angle with water, θ, deg	water absorption capacity, %, wt/wt
PHB	Sucrose, 50 mM + SA, 30 mM/0 h	4.4 ± 0.5	71.7 ± 3.2	5.2	0	70.1 ± 2.6	1.62 ± 0.24
PHB-PEG	Sucrose, 50 mM + PEG 300, 150 mM/12 h	2.2 ± 0.4	34.2 ± 2.7	4.3	0.18	52.3 ± 7.5	3.97 ± 0.18

where t_0 is the flow time for the solvent, s; and t is the flow time for the polymer solution, s.

The molecular weight was calculated according to the Mark–Hauvink– Kuhn equation with the following coefficients:

$$[\eta] = 7.7 \times 10^{-5} \times M^{0.82}.$$

The accuracy of viscosity [η] measurements was ~1%. The accuracy of molecular mass assessment according to the Mark–Hauvink–Kuhn equation was 2–5% [17].

Production of experimental polymer film samples. Experimental polymer film samples (thickness 40 μm, diameter 30 mm) were produced for analysis of the physicochemical properties of the obtained PHB and PHB-PEG polymers. The polymer films were prepared from 2% (wt/vol) solutions of the respective polymers in chloroform by solvent evaporation on a glass surface. The sample weight as measured with an AL-64 scale (max = 60 g, d = 0.1 mg, Acculab, United States) was 61 ± 8 mg, and the film thickness as measured by a magnet meter was 38 ± 6 μm [5].

Polymer hydrophilicity assessment. The hydrophilicity of polymer film surfaces was inferred from the contact angle of wetting between a water drop and the polymer film surface. A digital Contact Angle Meter 110 VAC (Cole-Palmer, United States) was used for the measurements that yielded static wetting angle values for the surfaces. A drop of deionized distilled water (5 μL) from a microsyringe was placed on the surface of a polymer film attached to a coverslip, and the wetting angle of the film surface was measured by the photo camera of the device and specialized software. The Laplace–Young method was used to approximate the drop shape.

Water absorption by PHB and PHB-PEG polymer films was measured according to the standard (ISO U. 62: 2008) and calculated with the formula

$$\text{Water absorption } (\%) = (m_2 - m_0)/m_0 \times 100\%,$$

where m_0 and m_2 are the masses of dehydrated and water-saturated samples, respectively.

Film samples were dried at 50°C for 2–3 days to a constant weight (m_1) and immersed in deionized water at 25°C for 3 h. Water drops were removed, and the samples were weighed again. The treatment was continued until the mass increase dropped below 0.1 mg (m_2). The samples were dried again (50°C, 24 h) and weighed again (m_3). The values used in the calculations were the following: $m_1 = m_0$ at $m_1 < m_3$ and $m_3 = m_0$ at $m_3 < m_1$. The result is presented as the average (n = 3) [5].

Preparation of porous scaffolds. Double leaching, a novel modification of the leaching method widely used to create scaffolds in tissue engineering [18, 19], was used to prepare the porous scaffolds. A polymer solution in trichloromethane (ECOS-1, Russia; 60 mg/mL for PHB and 30 mg/mL for PHB-PEG) was mixed with ammonium carbonate (Khimmed, Russia) and sucrose (Sigma, United States) granules in a Petri dish. The solvent (chloroform) was allowed to evaporate, and the Petri dish was placed in hot water (~65°C) afterwards. Ammonium carbonate hydrolysis occurred at the first stage of leaching, and several rinses with water were performed at the second stage to ensure complete removal of sucrose. As a result, three-dimensional porous scaffolds composed of PHB and a PHB-PEG copolymer were obtained.

Analysis of polymer scaffold morphology. The general appearance of the scaffolds was visualized with the macrophotography function of a Cyber-shot DSC-RX100 photo camera (Sony, Japan). The morphology and structure of the scaffolds were characterized in a scanning electron microscopy (SEM) study on a JSM-6380LA device (Jeol, Japan) and in a wide-field light microscopy (WFSM) study on a Nikon SMZ1500 device (Nikon, Japan) [19]. The samples for SEM were gold coated in an IB-3 device (Giko, Japan) for 15 min at a current of 15 mA.

Analysis of polymer scaffold porosity. The scaffold porosity was inferred from the values of polymer weight in the sample. The first method for porosity (P) calculation used the formula

$$P = (1 - m_1/m_2) \times 100\%,$$

where m_1 is the porous sample weight and m_2 is the calculated weight of a nonporous monolithic sample with a volume equal to that of the porous sample (polymer density 1.25 g/cm^3).

Scaffold pore connectivity was assessed in an "ink test" that involved the staining of scaffold samples with ink. A sample was immersed in ink, dried, and cut open to demonstrate the absence of closed pores, which would appear as white spots on the cut surface [19].

BSA adsorption on polymer scaffolds. BSA (Sigma, United States) was used as the model protein in studies of protein adsorption on PHB and PHB-PEG scaffolds. The BSA adsorption experiment included the following stages: incubation of polymer scaffold samples (5 × 5 × 5 mm) in a protein solution (1.0 mg/mL in potassium phosphate buffer from Serva, Germany) at 37°C (in a thermostat) for 1 h and the subsequent transfer of the samples into potassium phosphate buffer and incubation under the same conditions (protein washout). This step was repeated three times (incubations I, II, and III) in order to attain complete washout of reversibly adsorbed protein; afterwards, the samples were transferred into distilled water to remove the buffer components. Samples used for the analysis of irreversibly adsorbed protein were transferred into a 0.01% aqueous solution of SDS and washed twice (incubations IV and V). The optical density (OD) of the solutions obtained during BSA desorption (incubations I, II, and III) was measured at 280 nm on an UV-1601PC spectrophotometer (Shimadzu, Japan).

Protein adsorption was also studied with samples incubated in potassium phosphate buffer with fluorescein isothiocyanate-labeled BSA (1 mg/mL, FITC-BSA, Sigma, United States) for 1 h at 37°C (in a thermostat). Nonadsorbed protein was removed by washing with potassium phosphate buffer, and the protein distribution on sample surface was assessed by laser scanning confocal microscopy (LSCM) on an LSM 710 device (Zeiss, Germany) at an excitation wavelength of 488 nm and a detection wavelength range of 493 to 634 nm. ImageJ software was used to analyze the images.

Circular dichroism (CD) spectra of the solutions of desorbed proteins were recorded on a Chirascan CD spectrometer (AppliedPhotophysics, Great Britain) [19].

Proliferation of COS-1 fibroblasts on polymer scaffolds. COS-1 African green monkey fibroblasts (Biolot, Russia) were used for in vitro assessment of scaffold biocompatibility. The cells were cultured in glucose-enriched (4.5 g/L) DMEM (Dulbecco's Modified Eagle Medium, Invitrogen, United States) with 10% fetal bovine serum (FBS), 100 MU/mL penicillin and 100 μg/mL streptomycin (Invitrogen, United States). The cells were incubated at 37°C and 5% CO_2, and the medium was exchanged once in 3 days. Fibroblasts were detached from the scaffolds by a trypsin-versene solution (0.05% trypsin and 0.02% versene in PBS, Serva, Germany) and counted in a Goryaev chamber [19].

The fibroblast proliferation on PHB and PHB-PEG scaffolds was studied in 96-well plates. Twelve samples of each polymer scaffold were placed in the plate wells and overlaid with cell suspension at 5000–6000 cells per well. The plates were incubated for 24, 48, and 120 h. A test based on the conversion of an insoluble tetrazolium salt into a soluble colored formazan salt by the active enzymes of cell mitochondria (XTT Cell Proliferation Kit, Biological Industries, Israel) was used to monitor cell survival and proliferation. The porous polymer films were carefully transferred to wells with 100 μL of fresh medium after 24, 48, or 120 h of incubation, 50 μL of XTT solution were added into each well, and the plates were incubated at 37°C for 2.5 h. The polymer scaffolds were removed from the wells and solution absorbance at 450 nm (reference wavelength 620 nm) was assessed in a Zenyth 3100 Microplate Multimode Detector (Anthos Labtec Instruments, Austria). The number of living cells was calculated according to a standard calibration curve for the XTT test [19].

RESULTS AND DISCUSSION

The parameters of PHB biosynthesis and bioPEGylation for PHB-PEG copolymer production are listed in Table 1. Supplementation of the cultivation medium of the producing *A. chroococcum* strain by PEG 300 suppressed biomass growth and enabled the production of a PHB-PEG copolymer that contained 0.18 mol % PEG. The PEG molecule is linked to the carboxyl group of the growing polymer chain and thus prevents further elongation of the chain and restricts the molecular weight increase; therefore, the PEG content attained points at the presence of a PEG moiety in virtually every PHB chain. The contact angle of wetting by water was significantly lower (25%) for the PHB-PEG copolymer as compared to the PHB copolymer, whereas the water absorption was higher (almost 2.5 times); this demonstrates a significant increase of hydrophilicity upon PHB-PEG copolymer production by PHB bioPEGylation.

We produced three-dimensional PHB and PHB-PEG scaffolds by double leaching. SEM and WFLM studies and ink tests (Fig. 1) of the polymer scaffolds showed that the scaffolds had a three-dimensional porous structure with an open interconnected network of pores. Pore size did not differ significantly between PHB and PHB-PEG scaffolds, as the micropore size was 22–23 μm and the macropore size was 400–600 μm. The average porosity was 93–94% for both types of scaffolds (Table 2). It is necessary to note that macropores of more than 300 μm in size are considered optimal for nutrient and cell penetration into the entire volume of the material, whereas microporosity is essential for cell attachment and growth in the scaffold [20]. Moreover, it was demon-

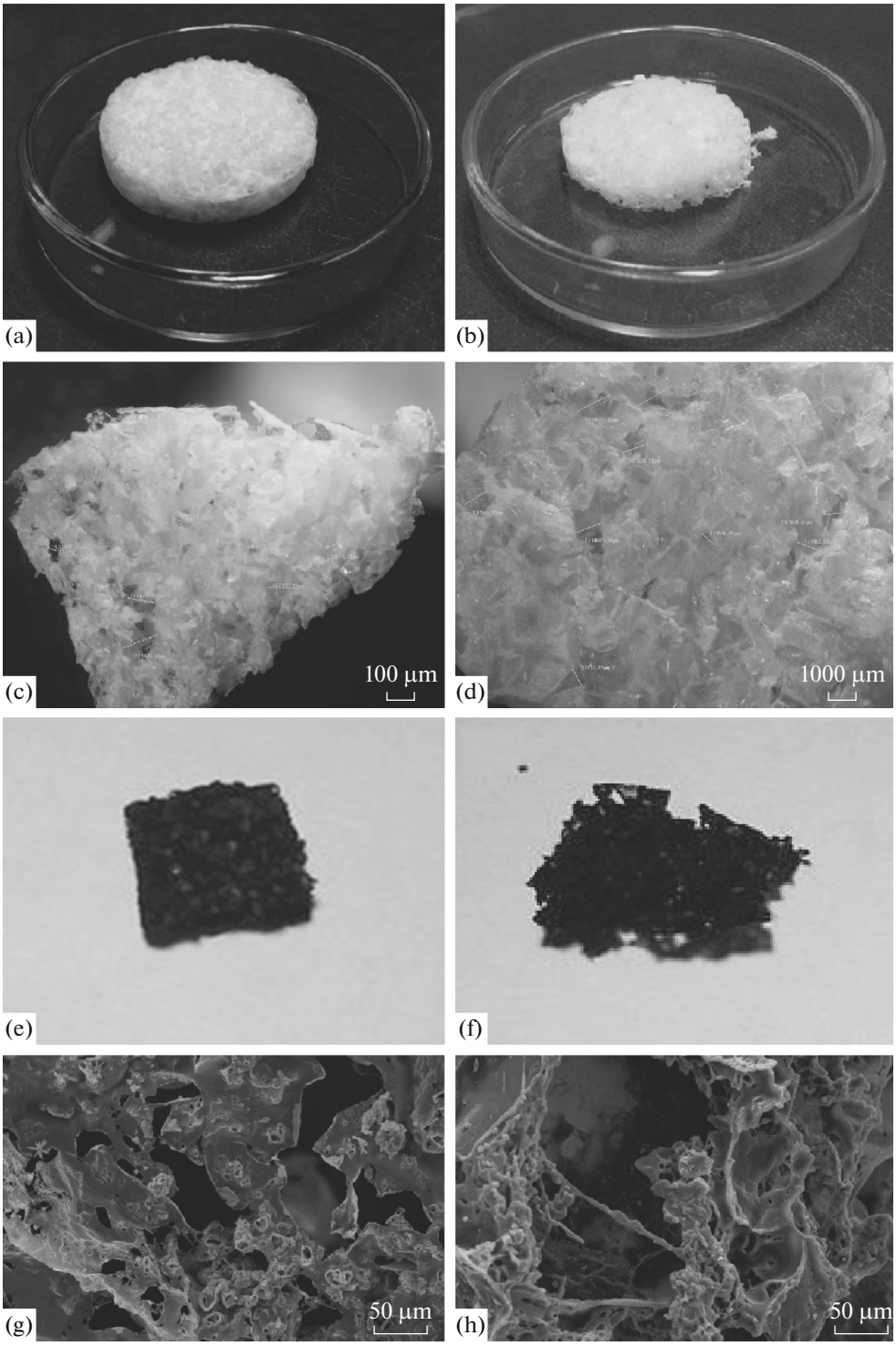

Fig. 1. Overall appearance and microstructure of PHB (a, c, e, g) and PHB-PEG copolymer (bioPEGylated; b, d, f, h) scaffolds. (a, b) overall appearance of the scaffolds; (c, d) scaffold microstructure, WFSM, ×100; (e, f) ink test, WFSM, ×100; (g, h) scaffold microstructure, SEM ×300.

strated earlier that dissolved BSA efficiently penetrated porous PHB constructs of this type [21].

Scaffold microstructure analysis did not reveal differences between PHB and PHB-PEG scaffolds, whereas BSA adsorption on the two types of scaffolds differed significantly. Incubation of the samples in a protein solution (1 mg/mL) caused protein adsorption on the surface of the studied scaffolds. The amount of

Table 2. Porosity of PHB and PHB-PEG scaffolds

Scaffold characteristics		Scaffold	
Polymer		PHB	PHB-PEG
Porosity, %		93 + 1	94 ± 2
Pore size, μm	micropores	23 ± 8	22 ± 9
	macropores	410 ± 75	615 ± 64

Table 3. BSA adsorption on PHB and PHB-PEG scaffolds

Parameter	Scaffold	
Polymer	PHB	PHB-PEG
Total protein adsorption, μg BSA/mg polymer	2.9 ± 0.1	6.4 ± 1.4
Irreversible adsorption, %	47 ± 5	33 ± 9

protein adsorbed on PHB-PEG was approximately twice higher than that for the PHB scaffold, and this finding initially appears to contradict the results of other studies that demonstrated decreased BSA absorption on polymer scaffolds upon polymer surface hydrophilization [11, 22, 23].

Sequential incubations of polymer scaffold samples in a buffer revealed considerable differences in BSA desorption from the surface of PHB and PHB-PEG scaffolds. Most of the protein was already desorbed from the scaffold surface during incubation I, and the degree of desorption from PHB-PEG scaffolds was higher. Further incubations of the PHB-PEG scaffolds caused protein desorption at each "washing" stage, whereas virtually no desorption of the protein from PHB scaffolds occurred, even in the presence of sodium lauryl sulfate (Fig. 2). Approximately half of the protein was irreversibly adsorbed on PHB scaffolds, whereas 2/3 BSA adsorption on bioPEGylated PHB scaffolds was reversible (Table 3), according to the presumed decrease of the share of irreversibly adsorbed protein in the case of polymer surface hydrophilization [11]. Strong irreversible BSA adsorption was confirmed by other researchers. Thus, the formation of a stable BSA crown around nanoparticles prepared from copolymer of PHB with 3-hydroxyhexanoate was demonstrated; crown formation occurred exclusively due to protein adsorption on the polymer surface of the nanoparticles and increased the stability of a nanoparticle dispersion manifold [24]. BSA adsorption on the surface of films composed of copolymer of PHB with 4-hydroxybutyrate was studied with quartz microscales. The weight of adsorbed BSA increased rapidly for approximately 10 min and later reached a plateau, regardless of subsequent washing of the film with a buffer solution, which is also indicative of largely irreversible adsorption of the protein [23]. PHB bioPEGylation may cause an increase of the number of protein adsorption sites on the polymer and a related increase in the total amount of adsorbed BSA. However, changes in the polymer surface conformation and an increase in its hydrophilicity rendered BSA adsorption on PHB-PEG largely reversible and minimized the occurrence of critical changes in the protein conformation upon adsorption.

CD analysis of desorbed BSA was performed to reveal the putative changes in the secondary structure of the protein. Since α-helices account for 70% of bovine serum albumin structure [25], the circular dichroism spectrum for this protein has the typical appearance of an α-helix spectrum. The difference between the spectra of control and experimental protein samples was assessed at 220 nm. Data processing revealed differences between the spectra of intact pro-

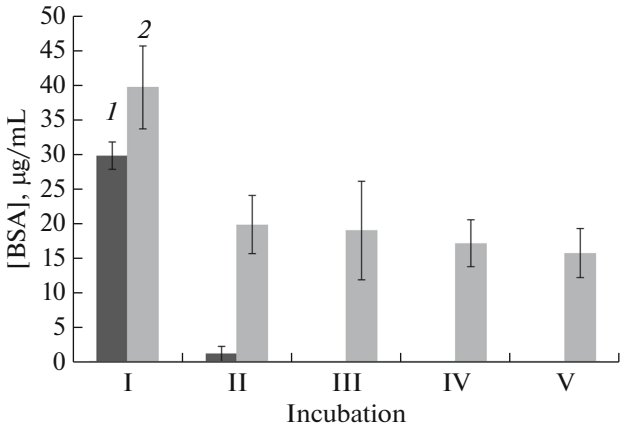

Fig. 2. Changes of BSA concentration in solution due to desorption from PHB (*1*) and PHB-PEG (*2*) scaffolds incubated in potassium phosphate buffer without a detergent (incubations I, II, and III) and in potassium phosphate buffer with 0.01% SDS (incubations IV and V).

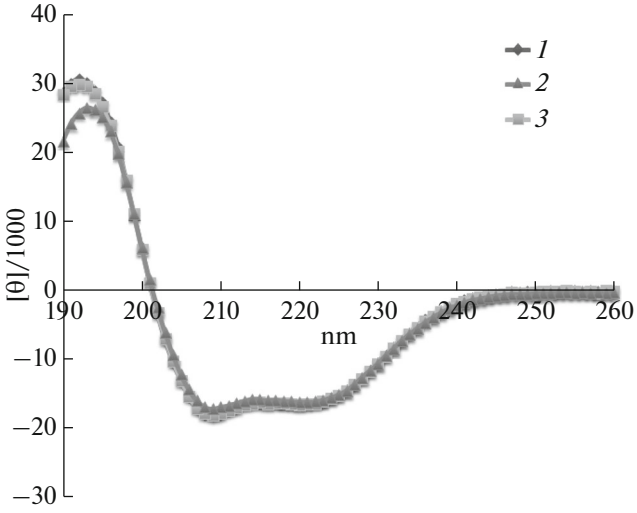

Fig. 3. CD spectra of intact BSA (*1*) and BSA desorbed from PHB (*2*) and PHB-PEG (*3*) scaffolds.

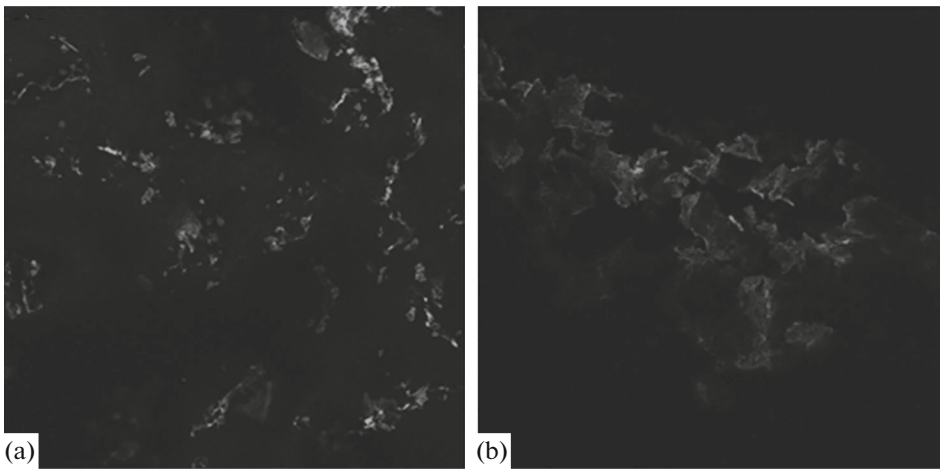

Fig. 4. Fluorescence microscopy images of FITC-BSA adsorbed on PHB (a) and PHB-PEG (b) scaffolds, ×400.

tein and protein desorbed from the scaffolds, but the difference was 3–4% and thus it remained within the limits of measurement error range (Fig. 3).

A qualitative demonstration of BSA adsorption was performed in a fluorescence microscopy study with FITC-BSA, a molecule with a fluorescent label. Figure 4 shows that the protein covered the pore surfaces in both scaffolds after washes with a buffer solution and sometimes formed "brighter" conglomerates that were more abundant on the surface of PHB scaffolds (Fig. 4).

The relationship between protein adsorption and cell growth on polymer scaffolds was assessed in a study of fibroblast (soft connective tissue cell) proliferation on PHB and PHB-PEG scaffolds. The data obtained demonstrated cell survival and active proliferation on the scaffolds during one week. There were no significant differences between fibroblast growth rates on scaffolds composed by different polymers, but a trend toward more intensive growth of cells on bioPEGylated PHB scaffolds was observed (Fig. 5).

Thus, bioPEGylation led to an increase of overall adsorption accompanied by a significant decrease of the share of protein irreversibly adsorbed on PHB-PEG polymer scaffolds, and this could have promoted better growth of fibroblasts on these scaffolds. Therefore, these scaffolds are better adapted for soft connective tissue reconstruction than PHB scaffolds.

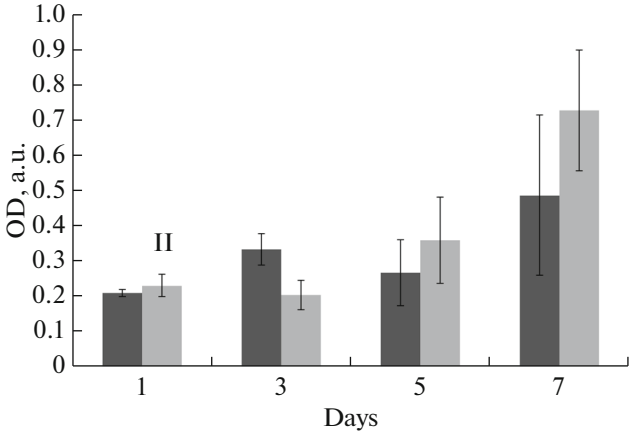

Fig. 5. Growth of COS-1 fibroblasts on PHB (I) and PHB-PEG (II) scaffolds.

ACKNOWLEDGMENTS

Financial support for the present work was provided by the Russian Science Foundation, grant no. 17-74-20104. Equipment available at the Collective Use Centers (core facilities) of Moscow State University (including a complex for polymer micro- and nanoparticle production) and Federal Research Centre "Fundamentals of Biotechnology" of the Russian Academy of Sciences) was used in the study.

REFERENCES

1. Lim, J., You, M., Li, J., and Li, Z., *Mater. Sci. Eng. C Mater. Biol. Appl.*, 2017, vol. 79, pp. 917–929.
2. Bonartsev, A.P., Bonartseva, G.A., Shaitan, K.V., and Kirpichnikov, M.P., *Biomed. Khim.*, 2011, vol. 57, no. 4, pp. 374–391.
3. Chan, R.T., Marcal, H., Ahmed, T., Russell, R.A., Holden, P.J., and Foster, L.J.R., *Polymer Int.*, 2013, vol. 62, no. 6, pp. 884–892.
4. Dominguez-Diaz, M., Meneses-Acosta, A., Romo-Uribe, A., Pena, C., Segura, D., and Espin, G., *Eur. Polym. J.*, 2015, vol. 63, pp. 101–112.
5. Bonartsev, A.P., Yakovlev, S.G., Zharkova, I.I., Boskhomdzhiev, A.P., Bagrov, D.V., Myshkina, V.L., Makhina, T.K., Kharitonova, E.P., Samsonova, O.V., Feofanov, A.V., Voinova, V.V., Zernov, A.L., Efremov, Yu.M., Bonartseva, G.A., Shaitan, K.V., and

Kirpichnikov, M.P., *BMC Biochem.*, 2013, vol. 14, p. 12.

6. Bonartsev, A.P., Zharkova, I.I., Yakovlev, S.G., Myshkina, V.L., Mahina, T.K., Voinova, V.V., Zernov, A.L., Zhuikov, V.A., Akoulina, E.A., Ivanova, E.V., Kuznetsova, E.S., Shaitan, K.V., and Bonartseva, G.A., *Prep. Biochem. Biotechnol.*, 2017, vol. 47, no. 2, pp. 173–184.
7. Chan, R.T., Russell, R.A., Marcal, H., Lee, T.H., Holden, P.J., and Foster, L.J., *Biomacromolecules*, 2014, vol. 15, no. 1, pp. 339–349.
8. Cheng, G., Cai, Z., and Wang, L., *J. Mater. Sci. Mater. Med.*, 2003, vol. 14, no. 12, pp. 1073–1078.
9. Nemets, E.A., Efimov, A.E., Egorova, V.A., Tonevitsky, A.G., and Sevastianov, V.I., *Bull. Exp. Biol. Med.*, 2008, vol. 145, no. 3, pp. 371–373.
10. Monnier, A., Rombouts, C., Kouider, D., About, I., Fessi, H., and Sheibat-Othman, N., *Int. J. Pharm.*, 2016, vol. 513, nos. 1–2, pp. 49–61.
11. *Biosovmestimye materialy: Uchebnoe posobie* (Biocompatible Materials: A Textbook), Sevast'yanov, V.I. and Kirpichnikov, M.P., Eds., Moscow: Med. Inform. Agentstvo, 2011.
12. Reusch, R.N., *Med. Hypotheses*, 2015, vol. 85, no. 6, pp. 1041–1043.
13. Pavlova, E.R., Bagrov, D.V., Kopitsyna, M.N., Shchelokov, D.A., Bonartsev, A.P., Zharkova, I.I., Mahina, T.K., Myshkina, V.L., Bonartseva, G.A., Shaitan, K.V., and Klinov, D.V., *J. Appl. Polym. Sci.*, 2017, vol. 134, p. 45090.
14. Atkins, T.W. and Peacock, S.J., *J. Biomater. Sci. Polym. Ed.*, 1996, vol. 7, no. 12, pp. 1065–1073.
15. Baran, E.T., Ozer, N., and Hasirci, V., *J. Microencapsul.*, 2002, vol. 19, no. 3, pp. 363–376.
16. Zhu, X.H., Wang, C.H., and Tong, Y.W., *J. Biomed. Mater. Res. A*, 2009, vol. 89, no. 2, pp. 411–423.
17. Myshkina, V.L., Nikolaeva, D.A., Makhina, T.K., Bonartsev, A.P., and Bonartseva, G.A., *Appl. Biochem. Microbiol.*, 2008, vol. 44, no. 5, pp. 482–486.
18. Kundu, J., Pati, F., Hun Jeong, Y., and Cho, D.W., in *Biomaterials for Biofabrication of 3D Tissue Scaffolds. Biofabrication: Micro- and Nano-Fabrication, Printing, Patterning and Assemblies*, Forgacs, G. and Sun, W., Eds., Oxford, UK: Elsevier, 2013, pp. 23–46.
19. Bonartsev, A.P., Zharkova, I.I., Yakovlev, S.G., Myshkina, V.L., Makhina, T.K., Zernov, A.L., Kudryashova, K.S., Feofanov, A.V., Akulina, E.A., Ivanova, E.V., Zhuikov, V.A., Volkov, A.V., Andreeva, N.V., Voinova, V.V., Bonartseva, G.A., Shaitan, K.V., and Kirpichnikov, M.P., *J. Biomater. Tissue Eng.*, 2016, vol. 6, no. 1, pp. 42–52.
20. Karageorgiou, V. and Kaplan, D., *Biomaterials*, 2005, vol. 26, no. 27, pp. 5474–5491.
21. Bian, Y.Z., Wang, Y., Aibaidoula, G., Chen, G.Q., and Wu, Q., *Biomaterials*, 2009, vol. 30, no. 2, pp. 217–225.
22. Venault, A., Subarja, A., and Chang, Y., *Langmuir*, 2017, vol. 33, no. 9, pp. 2460–2471.
23. Zhan, J., Wang, L., Liu, S., Chen, J., Ren, L., and Wang, Y., *ACS Appl. Mater. Interfaces*, 2015, vol. 7, no. 25, pp. 13876–13881.
24. Peng, Q., Wei, X.Q., Yang, Q., Zhang, S., Zhang, T., Shao, X.R., Cai, X.X., Zhang, Z.R., and Lin, Y.F., *Int. J. Nanomedicine*, 2015, vol. 10, no. 2, pp. 205–214.
25. Kulikova, T., Akhtar, R., Aldebert, P., Althorpe, N., Andersson, M., Baldwin, A., Bates, K., Bhattacharyya, S., Bower, L., Browne, P., Castro, M., Cochrane, G., Duggan, K., Eberhardt, R., Faruque, N., Hoad, G., Kanz, C., Lee, C., Leinonen, R., Lin, Q., Lombard, V., Lopez, R., Lorenc, D., McWilliam, H., Mukherjee, G., Nardone, F., Pastor, M.P., Plaister, S., Sobhany, S., Stoehr, P., Vaughan, R., Wu, D., Zhu, W., and Apweiler, R., *Nucleic Acids Res.*, 2007, vol. 35, suppl. 1, pp. D16–D20.

Translated by S. Semenova